



A PARAMETRIC ANALYSIS OF FUSED DEPOSITION MODELING PROCESS PARAMETERS WITH REFERENCE TO MECHANICAL PROPERTIES OF THERMOPLASTICS

Ravi Shekhar Kinja

Dr. Kailash Chaudhary

Dr. Dinesh Shringi

Abstract

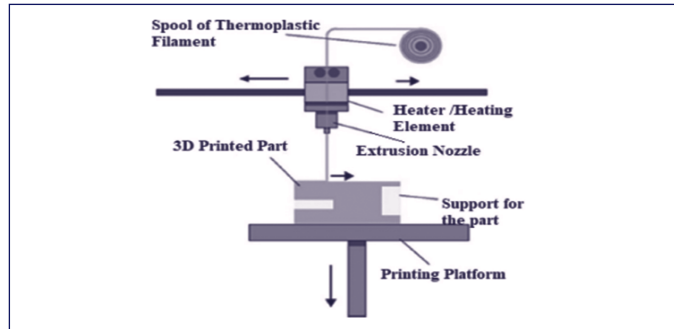
Fusion Modeling is a subset of additive manufacturing that uses CAD files to create a product. Additive manufacturing is widely used for prototype and low-volume production because of its durability, cost-effectiveness, safe and efficient operation, and ability to manage high-quality thermoplastics. Given its potential to facilitate the construction of functional components with complicated geometry, fused deposition modeling (FDM) has emerged as a viable additive manufacturing technique offering an alternative to traditional fabrication methods. It is possible to control the mechanical qualities of a manufactured product by adjusting many process factors. The purpose of this research is to better understand how a desktop 3D printer's build orientation, layer thickness, and fibre volume content affect the mechanical performance of continuous fibre-reinforced composites. The mechanical response of the printed specimens is measured by performing tensile and three-point bending tests. Broken surfaces captured by a scanning electron microscope (SEM) are analyzed to ascertain the role that process factors play in the emergence of failure modes. In most situations, the findings reveal that strength and stiffness improve with a rise in fibre volume content, although the amount of improvement in mechanical performance does not.

Keywords: AM (Additive Manufacturing), 3D Printing, Mechanical Properties, Overhang angles, and Mechanical testing.

1. INTRODUCTION

Additive manufacturing (AM) utilizes CAD data to build products layer by layer. In contrast to typical manufacturing processes, AM builds three-dimensional items by layering material. This enables AM to print complicated, artificial components faster and cheaply. 3D printing doesn't need specific equipment, creates little waste, can print complex structures at high resolution, and allows for product customization and flexibility, making AM manufacturing faster and more efficient. AM technique Fused Deposition Modeling (FDM) is common. Scott Crump, Stratasys' co-founder, invented the FDM process in 1989. FDM uses thermoplastic filament to layer-print the component. Additive manufacturing may layer-by-layer construct an object from a CAD file. Layering raw materials makes 3D goods cheaper and quicker than conventional production. Inkjet modeling (IJM), selective laser sintering (SLS), 3D printing, DMD, FDM, and stereo lithography are commercial additive manufacturing technologies [1].

Figure 1. FDM process [2].



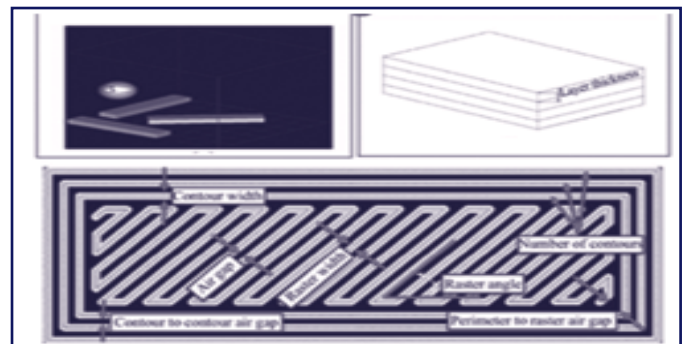
1.1 Fused Deposition Modeling (FDM) Process

Figure 1 illustrates the FDM process: the liquefying head warms a continuous filament of material to a semi-liquid condition, which is subsequently extruded onto the printing bed/platform. Fused deposition modeling (FDM) uses semi-liquid thermoplastic filament materials that fuse at ambient temperature to form layer-wise layered objects [2].

1.2 Fused Deposition Modeling (FDM) Parameters

Figure 2 describes several FDM process parameters. These are also key factors:

Figure 2. (a)Build orientation



(b) layer thickness

(c) FDM tool path parameter [3]

- The build platform's X, Y, and Z axes indicate the part's construction orientation, as shown in Figure 2a.

- Nozzle tip layer thickness is shown in Figure 2b. Layer thickness varies depending on material and tip size.
- An “air gap” arises between subsequent raster tool tracks on the same layer, as seen in Figure 2c.

2. LITERATURE OF REVIEW

There is a wide range of authors who have given their findings which are given below in table 1.

Table 1. FDM Technique Literature

Authors	Technique used	Outcomes
Enemuoh et al., (2021) [4]	ANOVA	The results show that the predicted hardness and tensile strength properties were adequately maximized while the energy consumption, production time, part weight, and dimensional changes were adequately minimized at the optimized control factor levels.
Awasthi et al., (2021) [5]	FDM	The FDM approach facilitates fast prototyping, individualized design, and extensive customization of TPEs. When compared to conventional molding techniques.
Penumakala et al., (2020) [6]	FDM	Mechanical properties of printed objects can be estimated using analytical and numerical models that simulate the FDM printing process.
Bakir et al., (2020) [7]	FDM	FDM-printed rPET constructions are acceptable for load-bearing applications because optimum process parameters provide strength and modulus values comparable to injection-molded components.
Bahr et al., (2018) [8]	FDM	The mechanical qualities of a road are significantly impacted by the sintering phenomena and crystallization at the contact.
Bhalodi et al., (2018) [9]	FDM	There is now a stronger connection between neck length growth, interface temperature, and time.
Chacon et al., (2017) [10]	FDM	Changes in mechanical qualities as a function of layer thickness and feed rate are insignificant, particularly for the on and flat orientations when the layer thickness is low.
Ning et al., (2017) [11]	FDM	Consequently, a fused deposition modeling machine is used to create carbon fiber-reinforced plastic composite components. To determine the tensile qualities, tensile tests are performed.

3. BACKGROUND STUDY

FFF layers of thermoplastic material using a nozzle. Complex

forms can't be created using current methods. Engineering materials outlast thermoplastics. FFF composite 3D printing feedstock's employing carbon fibres in a thermoplastic matrix for strength and stiffness are investigated in this study. Mark with mechanical qualities similar to unidirectional epoxy matrix composites, one printing of continuous carbon fibres surpasses unreinforced thermoplastics. Brittle continuous carbon fibres restrict design freedom. Short carbon microfiber filaments (~100 µm) print better than thermoplastic and may be used in traditional printing processes. FFF design freedom may be maintained with short fibre filaments with longer strands that have mechanical qualities similar to continuous fibre composites.

4. PROBLEM FORMULATION

Fused deposition modeling melts thermoplastic and extrudes it via a nozzle to make a three-dimensional object. Thermoplastic conditions enhance the component. To determine how fused deposition modeling process factors affect component attributes to extend component life to explain the relationship between process parameter variable operating points and mechanical performance. Experimentally verifying optimization results on test components reveals this study's goal.

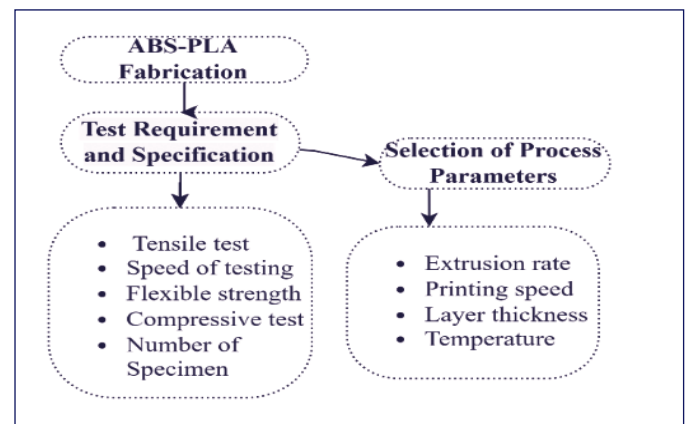
5. RESEARCH OBJECTIVE

- To reduce condensation before testing like the produced specimens.
- To better understand how process factors affect mechanical performance and clarify the results.
- Test specimens are created at two temperatures to determine how temperature influences test findings.

6. RESEARCH METHODOLOGY

Figure 3 shows the workflow of the methodology and contains various steps of ABS-PLA Fabrication.

Figure 3: Proposed methodology.



6.1 ABS-PLA Fabrication

Fused deposition modeling (FDM) is performed by using The APIUM P220 series FDM printer can print ABS-PLA, Polybenzimidazole (PBI), American Petroleum Institute (API), and Thermoplastic Polyimide (TPI) plastics, as well as severe temperature and technical plastics.

Figure 4. Apium P220 Series FDM printer [12]

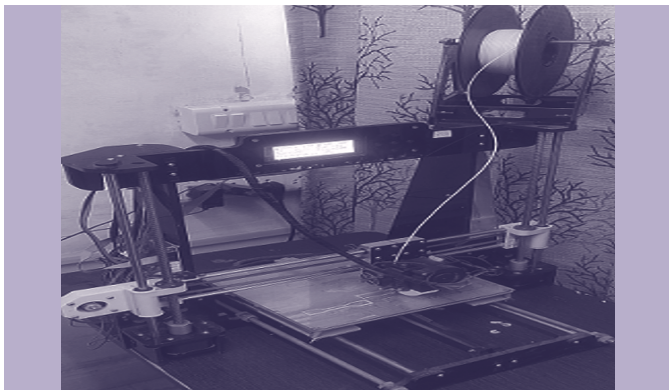


Table 2 shows the Polylactic Acid (PLA) and Acrylonitrile Butadiene Styrene (ABS), two plastics with distinct properties. Carbon fibre surrounds the ABS-PLA composite in this composition.[13]

Table 2. Material properties of PLA and ABS [14]

Properties	ASTM	Common material (PLA and ABS)	
Modulus of elasticity (MPa)	D 638-04	3750	26 2500-3000
Elongation at Break %	D 638-05	7	50
Load impact strength (J/m)	D 256-06	26	34
Color	-	Various	Various
Density (Kg/mm ³)	-	0.00105	0.00125
Tensile Strength (MPa)	D 638-03	59	40

6.2 Test Requirements specifications

Tensile and compressive tests are popular mechanical testing procedures for material functioning. Researching tensile and compressive mechanical behaviour yields material acreage data for element drawing and execution evaluations.

6.2.1 Tensile test

Specimen dimensions: narrow width 9.53 mm, thick length 6.35 mm, fillet radius 12.7 mm, overall width 3.40 mm. Figure 5 shows tensile test results.

Figure 5. Tensile test specimen and sizes. [15]



Displays sample structure and components. Tensile testing uses a 5mm/min crosshead speed regardless of material or application.

6.2.2 Compressive test

Compressive strength testing apparatus featured a crossheading speed of 1.3mm/min and a stack range of 50 KN. Here fixture holding the compression sample and compressive specimen. Prevents buckling and produces pure compression.

6.2.3 Number of Specimens

Three examples test ABS-PLA criteria and pricing. ASTM standards need five isotropic samples. However, research shows that three specimens, not five, are usually adequate for meaningful conclusions. Each experiment uses created specimens.

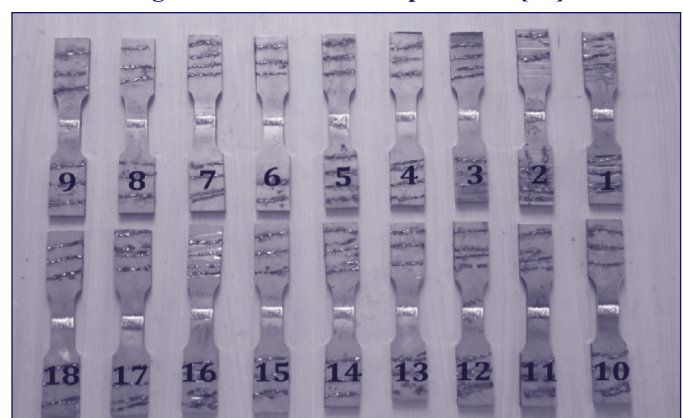
6.2.4 Speed of testing

If test features move at 5mm/min, stiffness testing will be problematic. Compression testing manipulates test matches at this pace.

6.2.5 Hardness Test

Brass, bronze, aluminum, and gold may be tested for Brinell's hardness. PLA was tougher and stiffer than ABS in Brinell hardness tests. Brinell hardness testers cannot be used on particularly hard or sensitive materials. The Brinell hardness number (BHN) test presses a steel ball of a thickness (F) against the test material's surface (F). After removing the weight, measure the indentation's average diameter (d) (P). BHN is computed by dividing the applied force P (in kilograms) by the indentation's spherical surface area A. [18]. Since the deformations caused by an indenter are similar to those seen in a tension test at ultimate tensile strength, many empirical connections between metals and alloys' hardness and engineering's ultimate tensile strength have been found. The bending test specimen is shown in Figure 6.

Figure 6. Hardness test specimens [20]



6.2.6 Flexible Strength

Flexural strength is a material's capacity to bend. Soft-flexible PLA's 92A shore hardness makes it flexible, unlike ordinary PLA, which is brittle. Due to their toughness, ABS fibres can sustain much.[21]

6.3 Selection of Process Parameters

There are various parameters that are selected for evaluation which are given as follows:

- Layer thickness
- Fill density
- Print Speed (mm/s)
- Print temp (°C)
- Nozzle size (mm)

7 RESULTS

Studying how processing factors impact mechanical attributes is crucial. Build orientation, extruder temperature, raster angle, layer height, infill percentage, and pattern affect the mechanical qualities of FDM-manufactured parts.

7.1 Results for both materials (PLA and ABS)

Tables 3 demonstrate PLA and ABS material's test results for physical and mechanical qualities.

Table 3 : Results of mechanical properties

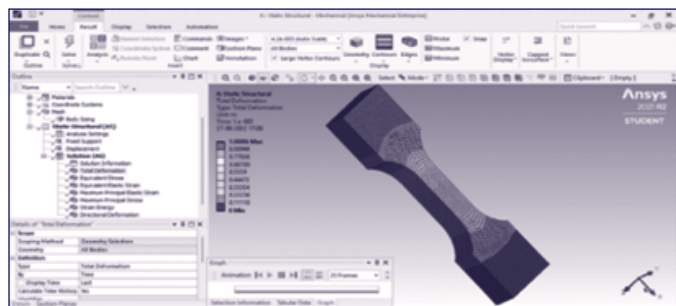
Sample	Specified Tests	Laboratory Results					
		1	2	3	1A	2A	3A
Polymer: PLA Specimen Process Fusion Deposition Modeling On 3D Printer	Tensile strength (N/mm ²)	15.05	22.28	27.85	26.49	24.07	22.88
	Compressive Strength (N/mm ²)	84.47	37.82	19.16	96.02	81.28	57.64
	Bending Strength (N/mm ²)	0.49	0.57	0.81	0.68	0.62	0.58
	Hardness Test Rockwell Hardness (HRC)	47	57	82	60	52	43
Polymer: ABS Specimen Process Fusion Deposition Modelling On 3D Printer	Tensile strength (N/mm ²)	22.28	28.06	37.33	27.10	18.43	12.64
	Compressive Strength (N/mm ²)	48.53	20.12	10.08	62.68	38.26	18.69 ²
	Bending Strength (N/mm ²)	0.80	0.85	0.88	0.73	0.65	0.58
	Hardness Test Rockwell Hardness (HRC)	8	13	38	104	98	85

7.2 Fusion Modeling of PLA and ABS

7.2.1 Based on Tensile Strength

A directional deformation coordinate system was created to predict the deformation direction, the highest principal stress, which matches ANSYS's main stress 1. The equivalent strain, which ignores hydrostatic stressing energy stored in a deformed body, is a shear strain measurement in the material. After an external force is removed, everything returns to normal. The total deformation shows all model distortions' X, Y, and Z-axis.

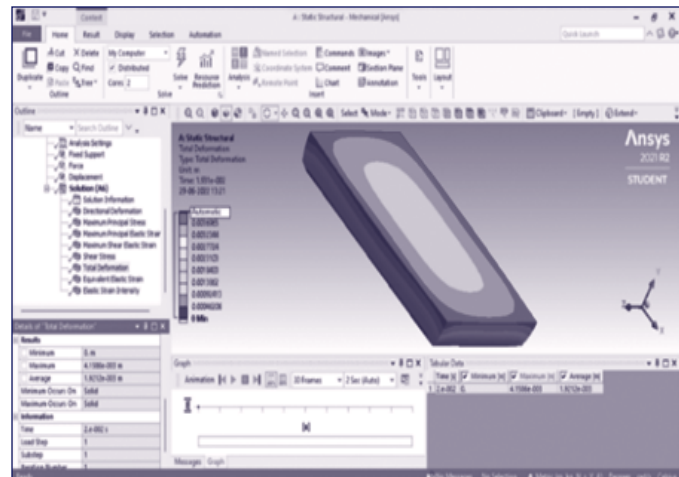
Figure 7: Shows the tensile strength properties of PLA and ABS fusion.



7.2.2 Based on Compression Testing

Stress and strain determine an object's interior strain energy. This model's deformation findings, including the equivalent stress of elasticity, maximum primary stress, meshing technique for continuous geometry, shear stress, and total deformation, may be shown in three dimensions using the complete deformation option (X, Y, and Z).

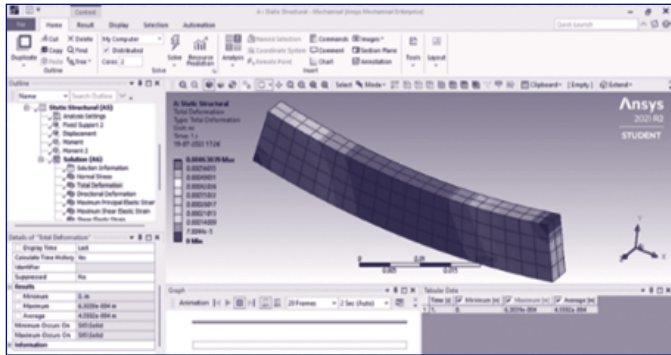
Figure 8: Shows the Compression Testing properties of PLA and ABS fusion



7.2.3 Based on the bending test

This examination standardized data collecting for R&D, specification validation, and quality control. Normal force, P, bends a beam or frame. The beam cannot recover after bending. Maximum elastic strain—the stress at which a material undergoes irreversible deformation—is connected to equivalent stress, the initial analysis setup (the analysis model's starting variables), the maximize elastic principle (elasticity is a deformable body's capacity), and the analysis model. Shear stress may not be largest along the neutral axis, the structure's maximum deformation, in the model-FG porous SMA/poroelastic composite cantilever beam bending model.

Figure 9: Shows the bending test properties of PLA and ABS fusion



7.2.4 Based on the hardness test

To perform the hardening test 8 samples are taken and each sample is tested 3 times and their harness values are recorded. Then from these 3 tested values of each sample an average hardness value is calculated as shown in table 4.

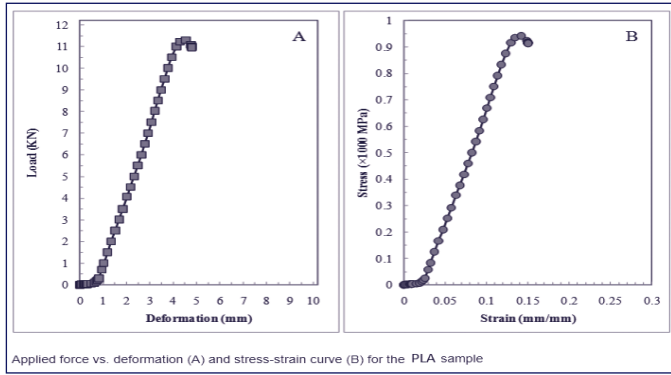
Table 4. Hardness test

Sample number	(Hardness (Rock well			Average hardness ((Rockwell
	Test 1	Test 2	Test 3	
1	43.0	44.3	42.3	43.20
2	37.2	35.6	42.5	38.43
3	63.3	61.0	61.4	61.90
4	56.0	53.4	54.8	54.73
5	63.7	62.9	62.9	63.17
6	54.2	55.7	59.9	56.60
7	61.3	61.7	63.7	62.23
8	52.5	52.4	49.8	51.57

7.2.5 Based on stress-strain and load and deformation for PLA material

Figure 10 illustrates the graphical representation between load or applied force (in KN) and deformation (in mm) along with a stress (in MPa) and strain (in mm) curves for samples of PLA material. It could be seen from the figure 10 (A) that a large amount of applied force would result in a very small amount of deformation and the curve shown in Figure 10 (B) depicts the relationship between stress and strain.

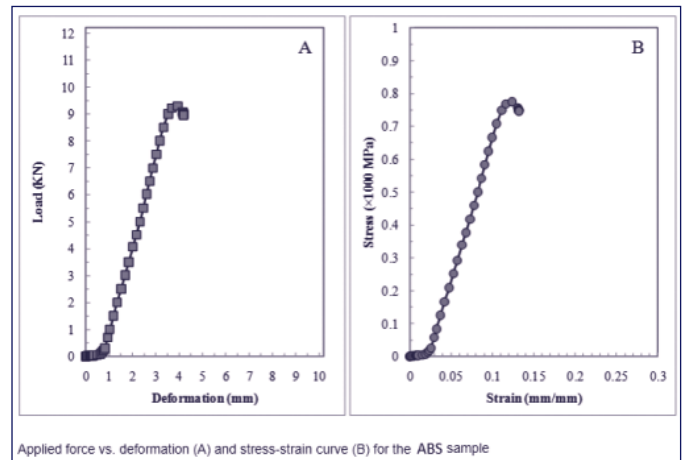
Figure 10. Applied force vs. deformation (A) and stress-strain curve (B) for the PLA sample



7.2.6 Based on stress -strain and load and deformation for ABS material

Figure 11 shows the graphical representation between load or applied force (in KN) and deformation (in mm) along with a stress (in MPa) and strain (in mm) curves for samples of ABS material. It could be seen from the Figure 11 (A) that a large amount of applied force would result in a very small amount of deformation and the curve shown in Figure 11 (B) depicts the relationship between stress and strain for ABS material.

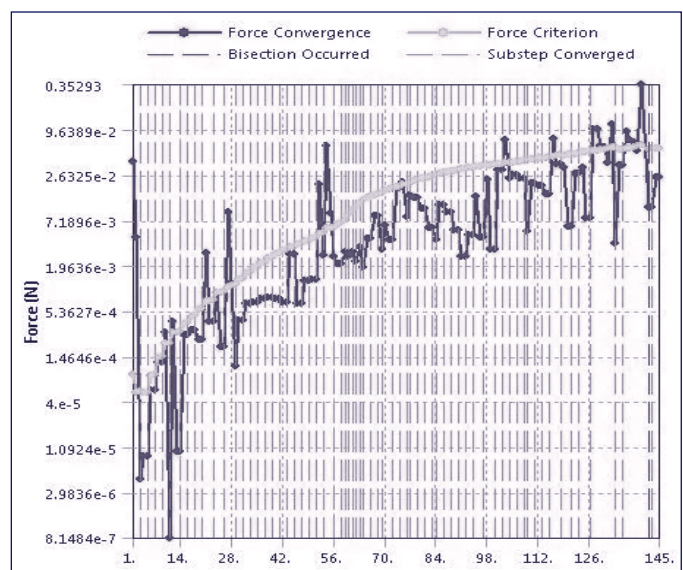
Figure 11. Applied force vs. deformation (A) and stress-strain curve (B) for the PLA sample



7.2.7 Based on simulation

Force convergence is the internal forces in each step. Figure 12 shows the graphical representation of convergence plot between force (N) with respect to time (in sec) of simulation results.

Figure 12. Force Convergence plot



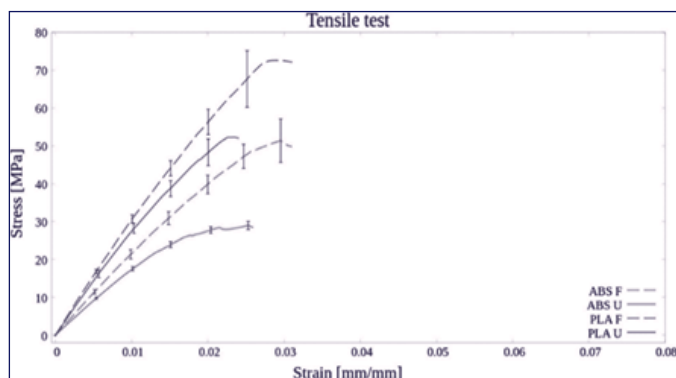
7.3 Comparison Graphs of PLA and ABS

F-Punch (the resulting change in momentum is proportional to its impulse). U-Punch Specimen (one atomic layer determines strength and ductility).

7.3.1 Based on Tensile Strength

Figure 13 depicts a trade-off between Stress (MPa) and Strain (mm) where PLA F and ABS F perform better than PLA U and ABS U. This depiction measures material tensile by parameters.

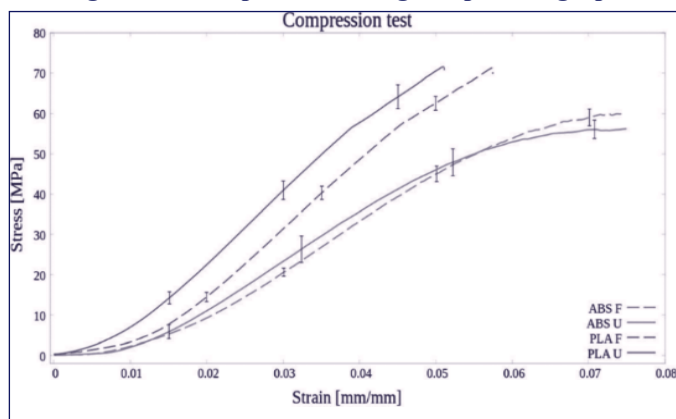
Figure 13: Tensile Strength comparison graph



7.3.2 Based on Compression Testing

Figure 14 demonstrates a trade-off between stress (in MPa) and strain (in mm) where PLA F and ABS F outperform PLA U and ABS U. This model measures compression by parameters for each material.

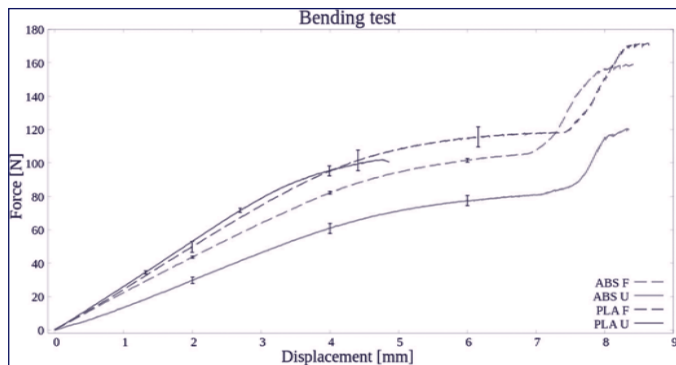
Figure 14: Comparison testing comparison graph



7.3.3 Based on the bending test

Figure 15 depicts a trade-off between Force (N) and Displacement (mm), with PLA F and ABS F outperforming PLA U and ABS U. This depiction is used to quantify material bending.

Figure 15: Bending test comparison graph



8. CONCLUSION AND FUTURE SCOPE

This research lists FDM process parameters and their impacts on FDM component dimensional accuracy, surface roughness, and finishing. Scholars employ AM methodologies and statistical optimization tools to discover which FDM process elements most affect a goal output, which parameters are crucial, and which parameters should be combined most efficiently. FDM process factors affect component quality and effectiveness, making this study crucial. FDM thermoplastics PLA and ABS are mainly explored. Build orientation, layer thickness, and fibre volume composition affected desktop 3D-printed continuous fibre-reinforced composite mechanical performance. Tensile and three-point bending tests evaluate printed specimen mechanics. According to the research, fibre volume content enhances strength and stiffness but not mechanical performance. FDM-printed CFRCs are immature. Vertical layer adhesion needs research. Only ABS, PLA, and nylon are low-temperature thermoplastics. Investigate impregnating high-temperature polymers over liquefier reinforcements. Two-nozzle printing polymers and reinforcements need tweaking.

REFERENCES

- 1 Mohamed, Omar A., Syed H. Masood, and Jahan L. Bhowmik. "Optimization of fused deposition modeling process parameters: a review of current research and future prospects." *Advances in manufacturing* 3, no. 1 (2015): 42-53.
- 2 Nikzad, Mostafa, S. Hasan Masood, and Igor Sbarski. "Thermo-mechanical properties of a highly filled polymeric composites for fused deposition modeling." *Materials & Design* 32, no. 6 (2011): 3448-3456.
- 3 Sheoran, Ankita Jaisingh, and Harish Kumar. "Fused Deposition modeling process parameters optimization and effect on mechanical properties and part quality: Review and reflection on present research." *Materials Today: Proceedings* 21 (2020): 1659-1672.
- 4 Enemuoh, Emmanuel U., Stefan Duginski, Connor Feyen, and Venkata G. Menta. "Effect of process parameters on energy consumption, physical, and mechanical properties of fused deposition modeling." *Polymers* 13, no. 15 (2021): 2406.
- 5 Awasthi, Pratiksha, and Shib Shankar Banerjee. "Fused deposition modeling of thermoplastic elastomeric materials: Challenges and opportunities." *Additive Manufacturing* 46 (2021): 102177.
- 6 Penumakala, Pavan Kumar, Jose Santo, and Alen Thomas. "A critical review on the fused deposition modeling of thermoplastic polymer composites." *Composites Part B: Engineering* 201 (2020): 108336.
- 7 Bakir, Ali Alperen, Resul Atik, and Sezer Özerinç. "Effect of fused deposition modeling process parameters on the mechanical properties of recycled polyethylene terephthalate parts." *Journal of Applied Polymer Science* 138, no. 3 (2021): 49709.
- 8 Bähr, Friedrich, and Engelbert Westkämper. "Correlations between influencing parameters and quality properties

of components produced by fused deposition modeling." *Procedia Cirp* 72 (2018): 1214-1219.

9 Bhalodi, Deep, Karan Zalavadiya, and Pavan Kumar Gurrala. "Influence of temperature on polymer parts manufactured by fused deposition modeling process." *Journal of the Brazilian Society of Mechanical Sciences and Engineering* 41, no. 3 (2019): 1-11.

10 Chacón, J. M., Miguel Angel Caminero, Eustaquio García-Plaza, and Pedro J. Núñez. "Additive manufacturing of PLA structures using fused deposition modelling: Effect of process parameters on mechanical properties and their optimal selection." *Materials & Design* 124 (2017): 143-157.

11 Ning, Fuda, Weilong Cong, Yingbin Hu, and Hui Wang. "Additive manufacturing of carbon fiber-reinforced plastic composites using fused deposition modeling: Effects of process parameters on tensile properties." *Journal of composite materials* 51, no. 4 (2017): 451-462.

12 Oosthuizen, Gert Adriaan, D. Hagedorn-Hansen, and T. Gerhold. "Evaluation of rapid product development technologies for the production of the prosthesis in developing communities." *Proceedings of SAIIE* 25 (2013).

13 Song, Yichi, et al. "Measurements of the mechanical response of unidirectional 3D-printed PLA." *Materials and design* 123 (2017): 154-164

14 <https://www.testresources.net/applications/test-types/tensile-test/thermoplastic-thermoset-plastics-tensile-testing/>

15 DAWOOD, Eethar Thanon, and Ali Jihad HAMAD. "Effect of NaCl on the Mechanical Properties of Structural Lightweight Concrete Reinforced with Fibers." *Walailak Journal of Science and Technology (WJST)* 14, no. 5 (2017): 389-399.

16 <https://markforged.com/resources/blog/pla-abs-nylon> access on 21/06/2021

17 Patil, Chetan, Hemant Patil, and Hiralal Patil. "Experimental investigation of hardness of FSW and TIG joints of Aluminium alloys of AA7075 and AA6061." *Frattura ed Integrità Strutturale* 10, no. 37 (2016): 325-332.

18 Sharma, Neeraj, Wathiq Sleam Abdullaah, Manish Garg, Rahul Dev Gupta, Rajesh Khanna, and Rakesh Chandmal Sharma. "Optimization of tig welding parameters for the 202 stainless steel using NSGA-II." *Journal of Engineering Research* 8, no. 4 (2020).

19 <https://www.allthat3d.com/pla-vs-abs/> access on 21/06/2021.

AUTHORS

Ravi Shekhar Kinja, Research Scholar, Department of Mechanical Engineering, MBM University Jodhpur, Air Force Area, Jodhpur – 342 011, (Rajasthan) India

Dr. Kailash Chaudhary, Assistant Professor, Department of Mechanical Engineering, MBM University Jodhpur, Air Force Area, Jodhpur – 342 011, (Rajasthan) India
Email: k.chaudhary.mech@gmail.com / 09829081113

Dr. Dinesh Shringi, Professor, Department of Mechanical Engineering, MBM University Jodhpur, Air Force Area, Jodhpur – 342 011, (Rajasthan) India